Available online at www.sciencedirect.com
ScienceDirect
Microelectronic Engineering 85 (2008) 175–180
MICROELECTRONIC ENGINEERING
www.elsevier.com/locate/mee

Fabrication of soft reflective microoptical elements using a replication process

Teng-Kai Shih [a,*], Jeng-Rong Ho [b], Jui-Hao Wang [a], Chia-Fu Chen [a,c], Chueh-Yang Liu [a], Chien-Chung Chen [d], Wha-Tzong Whang [a]

[a] Department of Materials Science and Engineering, National Chiao Tung University, 1001 Ta Hsueh Road, Hsinchu 300, Taiwan, ROC
[b] Graduate Institute of Opto-mechatronic Engineering, National Chung Cheng University, Chia-Yi 621, Taiwan, ROC
[c] Institute of Material and System Engineering, MingDao University, ChangHua 523, Taiwan, ROC
[d] Energy and Environment Research Laboratories, Industrial Technology Research Institute, Hsin Chu 310, Taiwan, ROC

Received 15 March 2007; accepted 7 May 2007
Available online 13 May 2007

Abstract

This paper reports the fabricated method and optical performance of soft, reflective elements with nonspherical surface. Based on excimer laser microdrilling and spin coating processes, a PMMA film suspended on microdrilled holes was used as a concave mold. Then, a high-reflectance material, mixed PDMS rubber polymers with TiO_2 nanoscale powders, was cast on the PMMA mold. Finally, both of concave and convex elements could be fabricated through soft replica molding processes and these elements could directly reflect light without the deposition of metal coatings. Therefore, we proposed a model regarding a flexible cable with its weight suspended on fixed points to explain the formation mechanism of PMMA molds. With the change of diameters of microholes and thicknesses of PMMA films, the suspended height of films was surely controllable. Therefore, the curvature radiuses and shapes of these aspherical elements also depended on the diameters of microholes and the thicknesses of PMMA films. Experimental results demonstrated that soft reflective elements have good surface qualities and high-quality optical properties. Besides, all fabrication steps can be executed in ambient environment and at low temperature, the proposed method has a potential for mass production.

Keywords: PDMS; Reflective elements; Nanoscale powders

1. Introduction

Micro-optical elements with their own scale of a few to several hundred micrometers are extensively applied to optical devices using MEMS technology to collect, distribute and modify optical radiation. In general, micro-optical elements can be roughly grouped into three generic areas; one is refractive, another is diffractive and the other is reflective. Refractive elements used in photoelectric systems are usually more popular than reflective ones. But reflective optics is useful for packaging an optical system into a smaller space than that which can be currently used for refractive optical elements [1]. Therefore, the optical characteristics of refractive elements depend mainly on the spectroscopic characteristics of photopolymerized resin used for its fabrication [1]. In order to eliminate this dependency, a reflective element could substitute for a refractive one and its optical performance was as good as that of a refractive element.

Generally speaking, reflective elements are essentially consisted of surface relief structures and metallic reflective coating. The focused ability of reflective elements mainly depends on surface relief structures and surface metal coatings. Therefore, various metal coatings could reflect light with a special region of wavelength. For example, silver films have a good reflectance in the whole visible spectrum and in the near-ultraviolet; gold films have a good

* Corresponding author. Tel.: +886 3 5712121x55346; fax: +886 3 5724727.
E-mail address: lifish20@yahoo.com.tw (T.-K. Shih).

0167-9317/$ - see front matter © 2007 Elsevier B.V. All rights reserved.
doi:10.1016/j.mee.2007.05.003

reflectance in the infrared region [2]. In past years, several technologies have been proposed to fabricate surface curved relief structures, such as self-surface tension method [3], diffusion-etching technology [4], gray lithography [5] and other fabricated technologies. For self-surface tension method and diffusion-etching technology, the fabricated relief formed always spherical surface due to the physical mechanism of fabricated technologies and this surface would lead spherical aberration when light was concentrated on the focused spot. In order to eliminate spherical aberration, an aspherical surface has been demonstrated to be able to improve effectively this disadvantage. One of most direct methods to form an aspherical surface is the use of gray lithography technology but this technology is very expensive. Hence, the first challenge is how to fabricate asperical surface structures using a simple and cheap technology.

With fast development of flexible devices, soft materials, polydimethylsiloxane (PDMS), have been paid much attention and have been used to fabricate various components [6–9]. In our previous work, the fabrication of PDMS microlens arrays using replica molding had been reported [7]. Therefore, we hope to develop additionally a reflective function under analogous fabrication processes. Although one of most direct approaches is that a metallic film deposited on the PDMS surface, a PDMS layer covered a metallic film would form spontaneously wavy structures on the PDMS surface due to the different contraction rates of cooling between the metal film and the PDMS layer [10]. These wavy structures on PDMS surface would cause the diffusion of light as light irradiated this surface. Therefore, metal films would easily crack under a small physical deformation due to the different ductility between the metal film and the PDMS layer. Hence, the secondary challenge is how to reflect light without metal films covered on the PDMS surface.

2. Experiment

Referring to the schematic depicted in Fig. 1, steps for fabricating soft reflective microoptical elements are described as follows:

(1) The footprint with designed shape and size for microoptical elements is defined on a metallic mask through which the excimer laser writes the footprint directly onto a polycarbonate (PC) plate. By monitoring the power intensity and number of laser shots, depth of the holes drilled by the excimer laser can be well controlled. Fig. 1a shows the resultant PC plate with microholes that serves as the pedestal in the next step.
(2) A thin liquid polymethylmethacrylate(PMMA) film is then coated on the PC-based pedestal through spin coating. As the liquid PMMA is rapidly spreading out, due to its weight and viscosity, a film, suspended on the pedestals and with special curvature, is formed on the pedestal. The schematic is shown in Fig. 1b. After baking at 60 °C for 5 min, the liquid film is solidified and stuck fixedly on the pedestal.
(3) A soft PDMS substrate with patterns with lens-like bump is fabricated by the replica molding method. Specifically, a liquid PDMS mixture, mixed nanoscale powders, silicone elastomer (Sylgard 184, Dow Corning) and corresponding curing agent, is cast onto the PMMA film obtained in Step 2. The weight percentage of powders in PDMS mixtures is about 20–30%. After baking at 60 °C for 20 min, the solidified PDMS polymers can be easily stripped from the PMMA film. The resulting PDMS structures are not only reflective elements but also master molds in next step. The resulting convex reflective element is shown in Fig. 1c.
(4) A concave element can be fabricated by a second replica molding process. The schematic is shown in Fig. 1d. To make sure both the concave and convex PDMS elements can be separated after baking, the weight ratio of the silicone elastomer and the curing agent for the concave mold should be different from that for the convex mold. In this study, the ratio for the concave mold is set at 5:1. The resulting concave reflective element is shown in Fig. 1e.

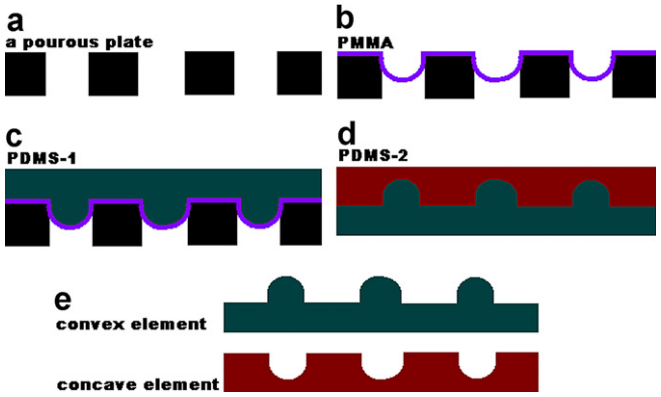

Fig. 1. Schematic for the fabrication processes of soft, reflective elements using a replication processes.

3. Results and discussions

3.1. The effect of metal films covered on an elastical substrate

When an Au film with the thickness of 100 nm was covered on a PDMS substrate with patterns of lens-like bump, wavy structures on this PDMS substrate could be found on Fig. 2. In our previous work, we have been indicated that wavy surface structures were formed on the PDMS substrate due to the different contraction rates of cooling between the Au film and the PDMS layer. The coefficients of thermal expansion of PDMS and Au are 960×10^{-6}/K and 14×10^{-6}/K, respectively. The large difference in volu-

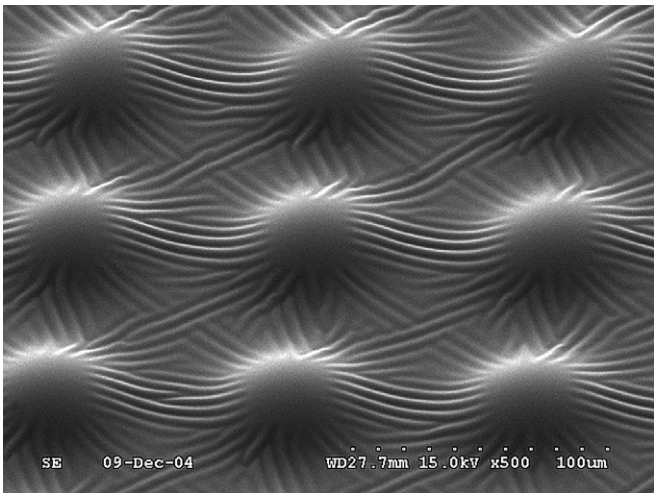

Fig. 2. The SEM image of wavy structures on the patterned surface of PDMS covered a metallic film with 100 nm thickness.

metric contraction rates introduced a compressive stress on the PDMS surface and led to the wavy surface structures [10]. To avoid the formation of wavy structures, PDMS mixtures used directly as a high-reflectance surface without a metal coating was discussed in next paragraph.

3.2. The preparation of soft reflective materials

Because most of photoelectric systems have a light source with a visible-light wavelength ranged between 350 and 700 nm, we hoped to get a high-reflectance material in the visible-light region. PDMS mixtures mixed with various kinds of nanoscale powder, including silica (SiO_2), titania (TiO_2), calcium carbonate ($CaCO_3$), zirconia (ZrO), zinc oxide (ZnO), and alumina (Al_2O_3) were respectively characterized by UV–vis spectrophotometer. Fig. 3a shows a reflectance curve of PDMS mixture polymers as a function of incident wavelength ranged between 200 nm and 1100 nm. Consequently, we found that the reflectance of TiO_2/ PDMS, which achieved 98%, was the most suitable candidate in these PDMS mixtures. The TiO_2/ PDMS mixtures could reflect most of visible light and its reflectance value was better than the value of traditional aluminum coatings (90%) using as reflective films. Hence, the PDMS/TiO_2 mixtures could substitute for metal coatings to reflect visible light.

It has been known that the processes of absorption, refraction, scattering and other interactions would occur as light illuminated on any matter. In this study, light can be reflected by PDMS mixtures, which is due to light scattering phenomenon. As PDMS mixtures in which nanoscale particles distributed uniformly were illuminated by light, particles would absorb light with a special energy and then excited electrons in particles released other types of radiation such as ultraviolet rays, visible light and infrared rays in all directions when excited electrons returned ground state. Hence, scattering processes can be simply

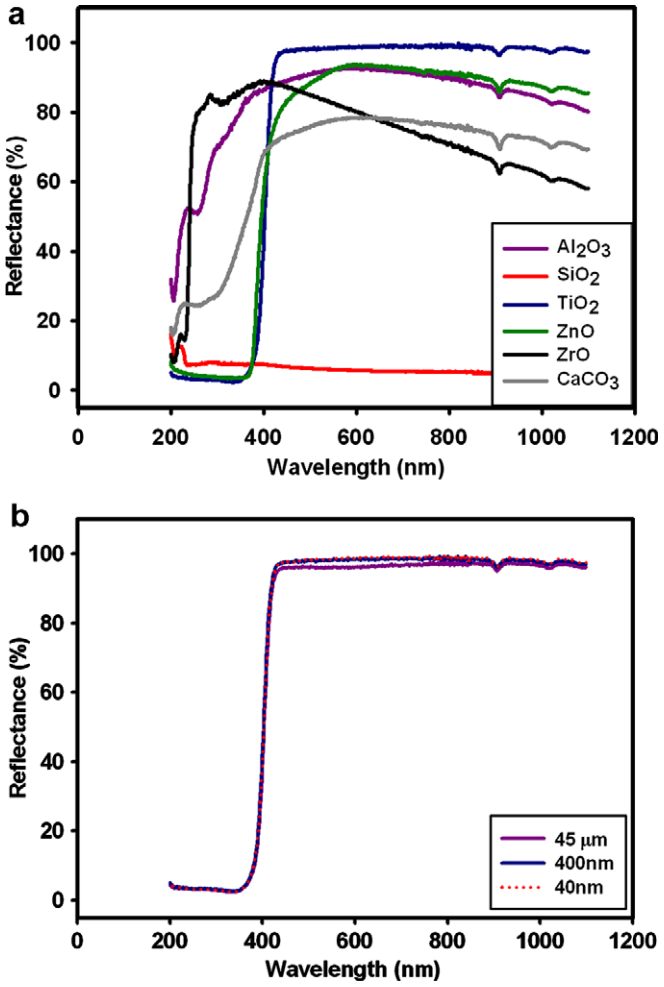

Fig. 3. (a) A reflectance curve of PDMS mixtures mixed with different powders as a function of incident wavelength ranged between 200 and 1100 nm. (b) A reflectance curve of TiO_2 with three sizes, $r = 40$ nm, 400 nm, and 45 μm/PDMS mixtures as a function of incident wavelength ranged between 200 and 1100 nm.

expressed as: scattering = excitation + reradiation [11]. In fact, light scattering processes involved many factors, such as the size and shape of particles, the type and property of materials and other corresponding factors etc. Additionally, the surface color of powders was also an important factor. For example, as the color of powders is close to white, it means that most of visible light is reflected; On the contrary, as the color of powders is black, it means most of light is absorbed.

Here, we adopted a simple model to explain experimental results. According to Rayleigh scattering formula, the intensity of light scattering can be roughly expressed as [11]:

$$I = \frac{8\pi^4 r^6}{\lambda^4}\left(\frac{n^2-1}{n^2+2}\right)^2(1+\cos^2\theta)$$

where r, n, λ, θ are the radius and refractive index of powders, wavelength and incident angle of light. The intensity of light scattering depended strongly on the size and refractive index of powders. Table 1 shows the refractive index

Table 1
The refractive index and color of various powders

Type of powders	TiO_2	ZnO	ZrO	$CaCO_3$	Al_2O_3	SiO_2
Refractive index of powders	2.76	2.02	2.17	1.58	1.7	1.55
Color of powders	White	Light yellow	White	Off-white	White	Translucent

and color of various powders. White TiO_2 powders have a larger refractive index than other materials in Table 1, causing to have the best reflectance for TiO_2/PDMS mixtures in Fig. 3a. Then, the size influence of TiO_2 powders was also considered. Fig. 3b shows a reflectance curve of TiO_2 with three sizes, $r = 40$ nm, 400 nm, and 45 μm, / PDMS mixtures as a function of incident wavelength ranged between 200 and 1100 nm. We found that the intensity of light scattering decreased slightly with the increase of particle size. Experimental results were contradicted with Rayleigh formula in which the intensity of light scattering was proportional to the six power of particle size. We observed that bigger particles in high-viscosity polymers would aggregate easily to form a bulk and such bulk would deposit on the bottom of PDMS. This aggregate phenomenon led the non-uniform distribution of particles and lowered the intensity of light scattering. Hence, the best fillers should be nanosize powders with a high refractive index.

3.3. The characters of the microoptical elements

Although we have presented experimentally some data regarding the tendency of a film suspended on the pedestals in previous work [7], an advancing model for the formation mechanism of a film with special curvature was addressed in this study. First, we simplified the problem of the curved PMMA film and introduced four assumptions into it. As a PMMA film was spread and covered on the porous PC plate, four assumptions were described here (1) every microhole on the PC plate is individual and there was no any interaction between each other; (2) a liquid film is immediately solidified and has no any ductility; (3) a PMMA film sticks strongly on the surface of the PC plate without slippage; (4) a three-dimensional condition is simplified to a two-dimensional one. Hence, the formation mechanism of a curve PMMA film should be similar to the model of a flexible cable with its weight suspended on fixed points [12]. In Step 2, the mass of a PMMA film itself was uniformly distributed on it and this film suspended on two points located on the same horizontal line. According to the cable model, the curved orbit of the PMMA film can be expressed through the following equation: $y = wx^2/2T$.

Parameters such as a distance between the lowest point and the horizontal roof of a curve (y), a diameter of a microhole (x), the mass of a film itself (w), and a inner tension of a film (T). Following this formula, the curve of a PMMA film, obtained in Step 2, depended mainly on the diameter of a microhole and the mass of a film itself. Table 2 shows the measured height of a suspended PMMA film obtained from different thickness of a PMMA film based on three diameters, with three kinds of different diameters, $x = 50$, 100 and 150 μm [7]. This model verified this proposed tendency that the suspended depth of a PMMA film increased with increasing the diameter of a microhole and the thickness of a PMMA film. Fig. 4 presents that the surface profile of a suspended PMMA film, measured by α-steper, can be closely fitted a parabolic shape and the fitting equation was expressed as: $y = ax^2 + bx + c$, where $a = 0.0076$, $b = -1.3807$, and $c = 44.6349$. However, the fitting equation was incompletely matched with the cable model. We suggested that the formation process of a curve film involved some rebellious problems. For instance, we did not know whether a liquid PMMA film would stretch during a cured process and the evaporation influence of a solvent existed in PMMA liquids. But this model still provided advancing information to understand the effect of controllable parameters and the explanation of a film with parabolic orbit.

Because the coefficient of thermal expansion of PDMS is quite small, replication structures cast against a suspended PMMA mold is faithfully replicated in Step 3. Fig. 5a and b shows the SEM images of a 2×2 convex

Table 2
The measure height of a suspended PMMA film obtained from different thickness of a PMMA film based on three diameters, with three kinds of different diameters, $x = 50$, 100 and 150 μm

The thickness of a PMMA films (μm)	The height of a microlens		
	$\Phi = 50$ μm	$\Phi = 100$ μm	$\Phi = 150$ μm
22	15.4	24.8	30.3
20	14.7	22.9	28.5
15	14.0	18.6	25.6
12	12.3	16.2	24.5

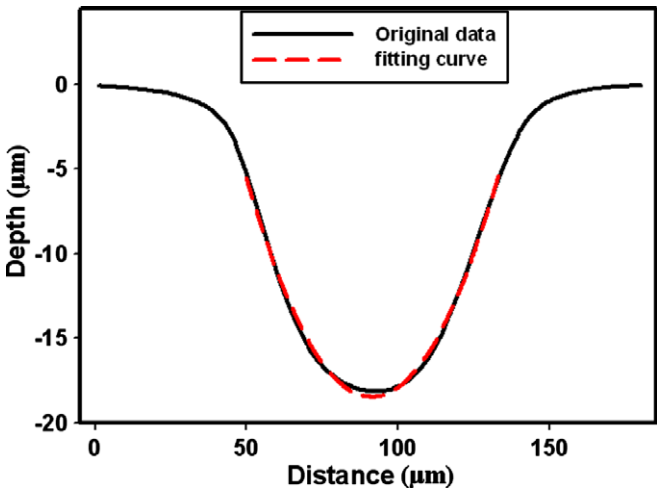

Fig. 4. The scanned profile of a suspended PMMA film through the measure of α stepper.

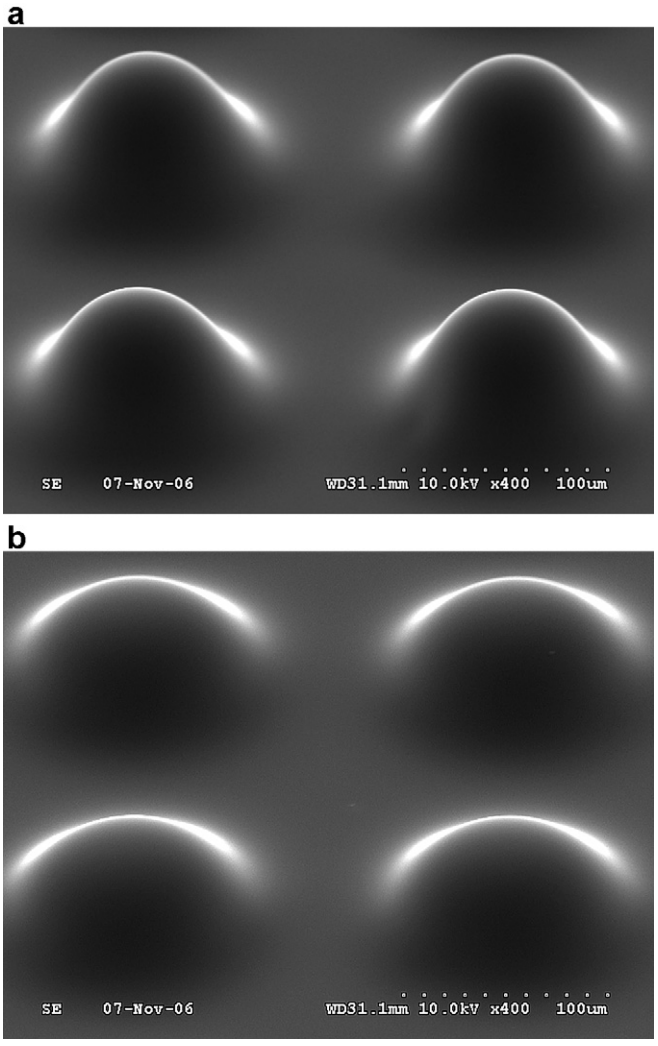

Fig. 5. SEM images for a 2×2 convex element array fabricated under different thickness of a PMMA film (a) 22 μm and (b) 12 μm.

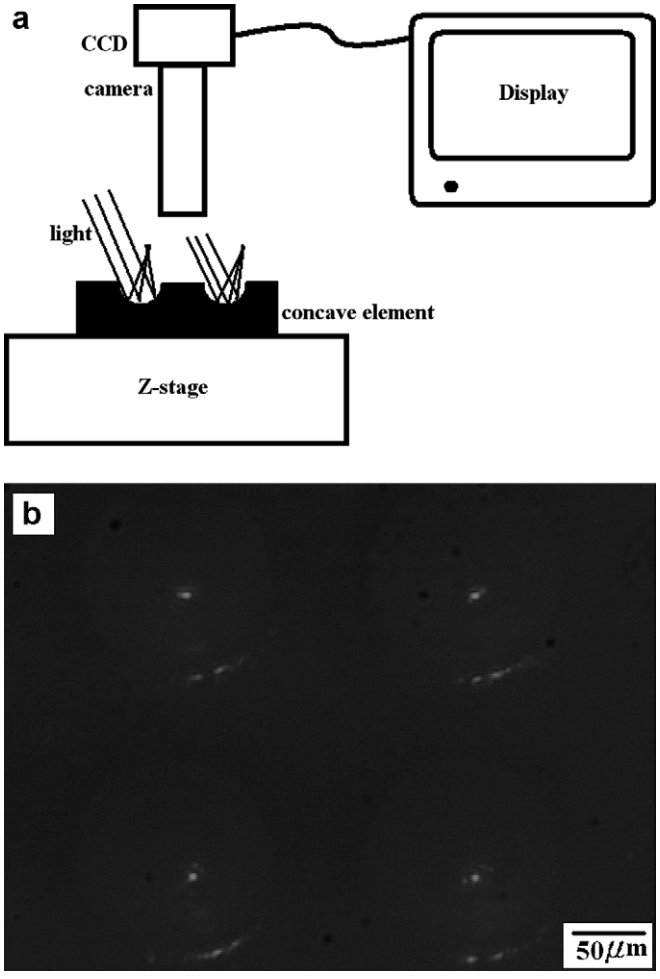

Fig. 6. Focused spot measurement: (a) schematic showing the experimental setup and (b) focused spot image.

element array with different heights. For an axial symmetrical plano-convex profile, the curvature radius (R) of a convex element can roughly be estimated through the following formula:

$$R = \frac{(K+1)h^2 + (\frac{\phi}{2})^2}{2h}$$

In this formula, ϕ and h is respectively the diameter and the height of a convex element, K is the aspherical constant [13]. The surface profile of a convex element is approximately parabolic shape, so K can take to be -1. Hence, the curvature radius of aspherical elements could still be controlled by the diameter of a microhole and the thickness of a PMMA film. After measuring by AFM, the root mean square surface roughness of a convex element in areas of 5×5 μm^2 was within 8 nm, corresponding to a total integrated scattering within 5% for visible light. This is because that the spin-coated PMMA film should be stayed in the liquid state for a reasonable time and with a certain film thickness so that the effect of the surface tension can modify the surface uniformity and lead a high-quality surface.

3.4. The optical property of reflective elements

The focusing property of the fabricated concave elements was examined experimentally. A schematic diagram of the experimental setup is shown in Fig. 6a. This setup consisted of a lamp as a white light source, microscope, CCD camera, image display and a micrometer scale resolution Z-stage. A 2×2 concave element with 100 μm diameter array was placed on the Z-stage and a lamp with a small inclined angle illuminated the surface of the concave element. The light would be focused on a spot by the reflection of concave surface structures. When the bright spot was arrived a minimal scale along the move of Z direction, this minimal spot was the focused spot of the concave element. The focused spots shown in Fig. 6b were about 4.2 μm. The other spots in Fig. 6b were due to the light reflected form the edge of the concave element. Hence, experiment results demonstrated fabricated concave elements are capable of generating spot arrays.

4. Conclusions

In this study, we have proposed a method to fabricate soft, reflective elements with nonspherical surface using a replication process. Based on excimer laser microdrilling, spin coating, and soft replica molding, both convex and concave elements can be fabricated. Replication structures made of high-reflectance materials (TiO_2/PDMS mixtures) could directly substitute for traditional reflective elements. With the increase of the diameters of microholes and the thicknesses of PMMA films, the heights of these elements were increased. Therefore, the curvature radiuses and shapes of these aspherical elements also depended on the diameters of microholes and the thicknesses of PMMA films. Experimental results shown soft reflective elements have good surface qualities and high-quality optical properties. Besides, all fabrication steps can be executed in ambient environment and at low temperature, the proposed method has a potential for mass production.

Acknowledgement

Financial support from the National Science Council of Taiwan under Grant No. NSC 95-2221-E-451-011 is gratefully acknowledged.

References

[1] Y. Awatsuji, M. Sasada, N. Kawano, T. Kubota, Jpn. J. Appl. Phys. 43 (2004) 5845–5849.
[2] M. Daniel, B.J. Thompson, Handbook of Optical engineering, Marcel Dekker, New York, 2001.
[3] Y. Weixing, X.C. Yuan, IEEE Photon. Technol. Lett. 15 (2003) 1410–1412.
[4] C.-S. Lee, C.-H. Han, Sens. Actuators A 88 (2001) 87–90.
[5] J. Yao, Z. Cui, F. Gao, Y. Zhang, Y. Guo, C. Du, H. Zeng, C. Qiu, Microelectron. Eng. 57–58 (2001) 729–735.
[6] M. Fleger, A. Neyer, Microelectron. Eng. 83 (2006) 1291–1293.
[7] T.-K. Shih, C.-F. Chen, J.-R. Ho, F.-T. Chuang, Microelectron. Eng. 83 (2006) 2499–2503.
[8] S. Moller, S.R . Forrest, J. Appl. Phys. 91 (2004) 3324–3327.
[9] D.A. Chang-Yen, R.K. Eich, J. Lightw. Technol. 23 (2005) 2088–2093.
[10] T.-K. Shih, C.-F. Chen, J.-R. Ho, C.-Y. Liu, F.-T. Chuang, Appl. Surf. Sci. 253 (2006) 2043–2049.
[11] C.F. Bohren, D.R. Huffman, Absorption and Scattering of Light by Small Particles, Wiley, 1983.
[12] J.L. Meriam, L.G. Kraige, Engineering Mechanics: Statics, Wiley, 1993.
[13] P. Nussbaum, R. Völkel, H.P. Herzig, M. Eisner, S. Haselbeck, Pure Appl. Opt. 6 (1997) 617–636.